Supporting Information

Molecular Engineering of Acoustic Protein Nanostructures

Authors: *Anupama Lakshmanan, Arash Farhadi, Suchita P. Nety, Audrey Lee-Gosselin, Raymond W. Bourdeau, David Maresca and Mikhail G. Shapiro.*

GV Variants	Midpoint of Collapse (P_c) (kPa)	P_c (SEM) (kPa)	ΔP (kPa)	ΔP (SEM) (kPa)	Adj. R-Square
ΔGvpC	195.30	0.27	17.01	0.24	0.999
ΔN&C	374.30	1.01	41.46	0.89	0.999
$GvpC_{WT}$	569.85	3.64	84.87	3.21	0.992

Table S1: Hydrostatic midpoint of collapse for engineered Ana GVs used in acoustic multiplexing experiments (Figure 2b). The data was fitted with a Boltzmann sigmoid function of the form $f(p) = \left(1 + e^{(p-p_c)/\Delta p}\right)^{-1}$ with p_c representing the average midpoint of collapse. Fit parameters and R^2 values for each of the GV variants are provided in the table.

GV Variants	Midpoint of Collapse (Pc) (kPa)	P_c (SEM) (kPa)	ΔP (kPa)	ΔP (SEM) (kPa)	Adj. R-Square
ΔGvpC	571.00	1.51	14.48	1.03	0.998
ΔN&C	657.04	3.94	77.47	3.70	0.997
$GvpC_{WT}$	868.81	6.56	94.00	5.57	0.994

Table S2: Acoustic midpoint of collapse for engineered Ana GVs used in multiplexing experiments (Figure 2c). The data was fitted with a Boltzmann sigmoid function of the form $f(p) = \left(1 + e^{(p-p_c)/\Delta p}\right)^{-1}$ with p_c representing the average midpoint of collapse. Fit parameters and R^2 values for each of the GV variants are provided in the table.

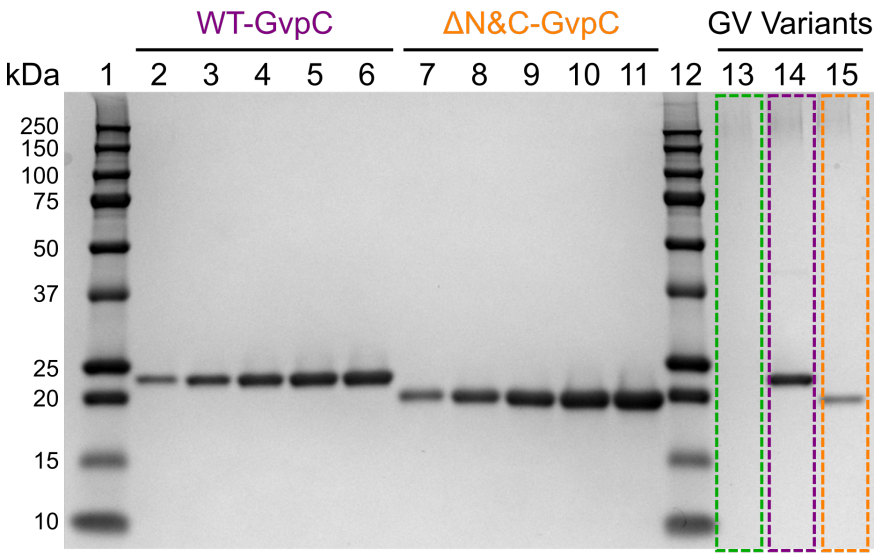

Lane	Sample
1	Ladder
2	WT-GvpC (200ng)
3	WT-GvpC (400ng)
4	WT-GvpC (600ng)
5	WT-GvpC (800ng)
6	WT-GvpC (1000ng)
7	ΔN&C-GvpC (200ng)
8	ΔN&C-GvpC (400ng)
9	ΔN&C-GvpC (600ng)
10	ΔN&C-GvpC (800ng)
11	ΔN&C-GvpC (1000ng)
12	Ladder
13	ΔGvpC Ana GVs (OD: 5)
14	$GvpC_{WT}$ Ana GVs (OD: 5)
15	ΔN&C Ana GVs (OD: 5)

Figure S1: SDS-PAGE analysis confirming the complete removal of GvpC from native Ana GVs (lane 13) and the re-addition of engineered proteins (lane 14-15). Quantification of re-added GvpC on urea-stripped Ana GVs was done by comparison against a standard curve (200 - 1000 ng) of the pure proteins

(lanes 2-6 for WT-GvpC and lanes 7-11 for ΔN&C-GvpC). The number of re-added GvpC molecules was determined to be ~ 1980 per GV for $GvpC_{WT}$ and ~ 877 per GV for ΔN&C respectively.

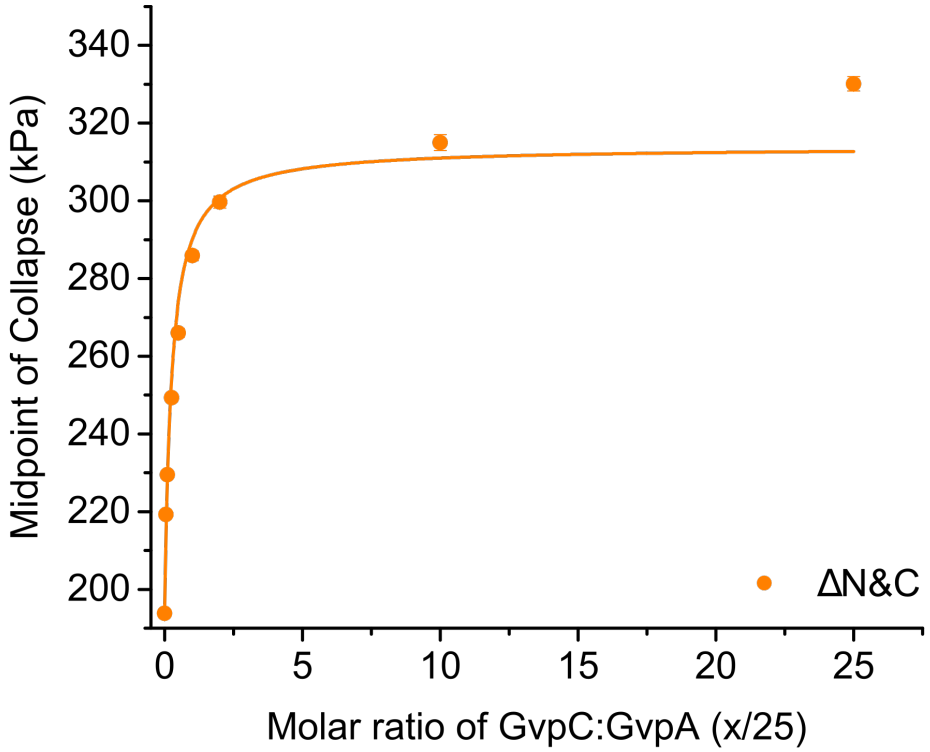

Molar ratio of GvpC : GvpA (x/25)	Midpoint of Collapse (Pc) (kPa)	P_c (SEM) (kPa)	ΔP (kPa)	ΔP (SEM) (kPa)	Adj. R-Square
0	193.77	0.31	16.72	0.27	0.999
0.05	219.29	0.46	20.44	0.40	0.999
0.1	229.47	0.62	21.9	0.55	0.999
0.25	249.28	0.99	28.07	0.88	0.998
0.5	266.01	1.13	30.94	0.99	0.998
1	285.85	1.19	33.95	1.05	0.998
2	299.66	1.53	40.31	1.35	0.997
10	314.99	2.01	50.84	1.77	0.996
25	330.11	1.88	50.75	1.65	0.997

Figure S2: Midpoint of collapse (hydrostatic) plotted as a function of re-added GvpC concentration for the ΔN&C variant. The midpoint of collapse was determined by fitting the raw data with a Boltzmann sigmoid function of the form $f(p) = \left(1 + e^{(p-p_c)/\Delta p}\right)^{-1}$ with p_c representing the average midpoint of collapse. Fit parameters and R^2 values for each of the GV variants are provided. The saturation curve was plotted by fitting the data to a bimolecular binding function of the form $f(x) = C_1 * x / (K_d + x) + C_2$.

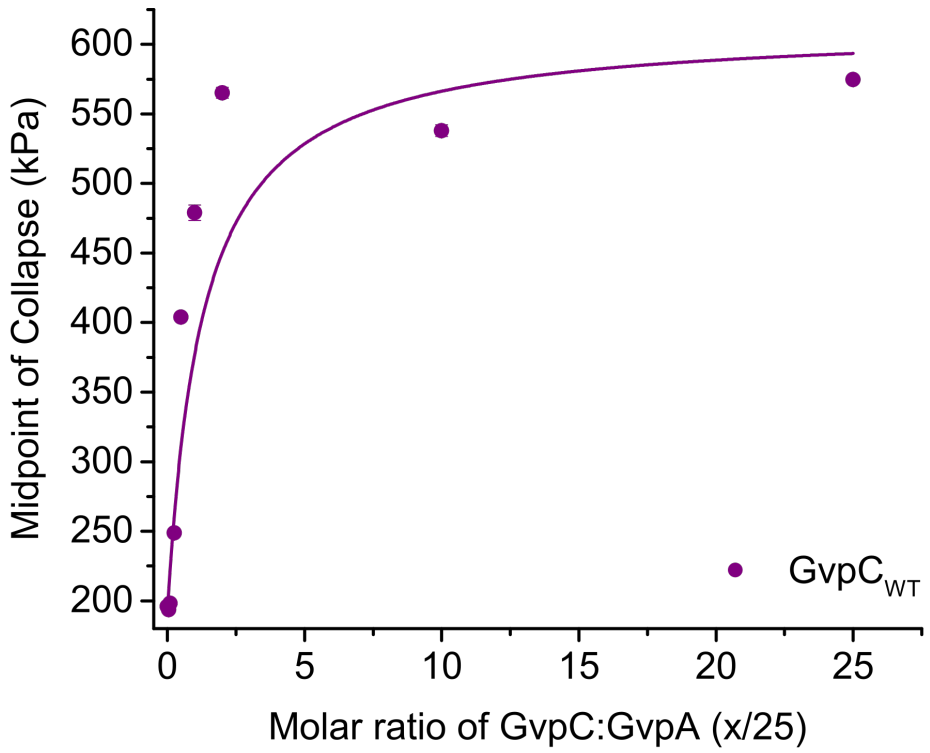

Molar ratio of GvpC : GvpA (x/25)	Midpoint of Collapse (Pc) (kPa)	P_c (SEM) (kPa)	ΔP (kPa)	ΔP (SEM) (kPa)	Adj. R-Square
0	195.95	0.21	16.23	0.18	0.999
0.05	193.48	0.43	17.54	0.38	0.999
0.1	198.12	0.91	19.90	0.80	0.998
0.25	248.68	1.24	33.60	1.09	0.998
0.5	403.93	2.24	61.03	1.98	0.996
1	479.01	5.50	108.11	4.88	0.985
2	565.15	3.92	79.10	3.46	0.990
10	537.95	4.24	86.97	3.74	0.989
25	574.72	2.29	62.93	2.03	0.996

Figure S3: Midpoint of collapse (hydrostatic) plotted as a function of re-added GvpC concentration for the GvpC$_{WT}$ variant. The midpoint of collapse was determined by fitting the raw data with a Boltzmann sigmoid function of the form $f(p) = \left(1 + e^{(p-p_c)/\Delta p}\right)^{-1}$ with p_c representing the average midpoint of collapse. Fit parameters and R^2 values for each of the GV variants are provided. The saturation curve was plotted by fitting the data to a bimolecular binding function of the form $f(x) = C_1 * x / (K_d + x) + C_2$.

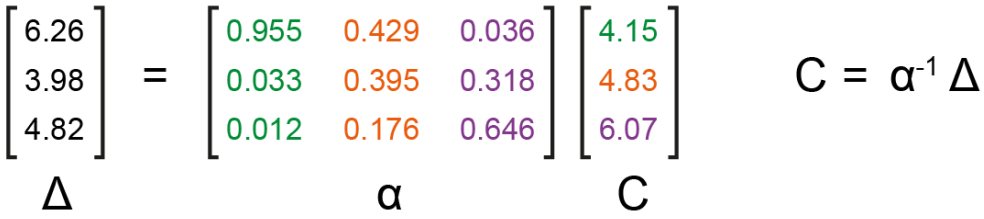

Figure S4: Matrix of coefficients used for generating spectrally unmixed images shown in Figure 2g from the pixel-wise ultrasound signal intensities in Figure 2f (I), before and after exposing the GV samples to three sequentially increasing acoustic pressures (P_i). Δ represents the measured differential signals with $\Delta_i = I(P_{i-1}) - I(P_i)$, while α is the matrix containing the acoustic collapse spectrum for each GV variant ($\alpha_{i,j}$). C represents the contribution of each GV variant to the observed signal, with C_j calculated by the matrix operation: $C = \alpha^{-1} \Delta$.

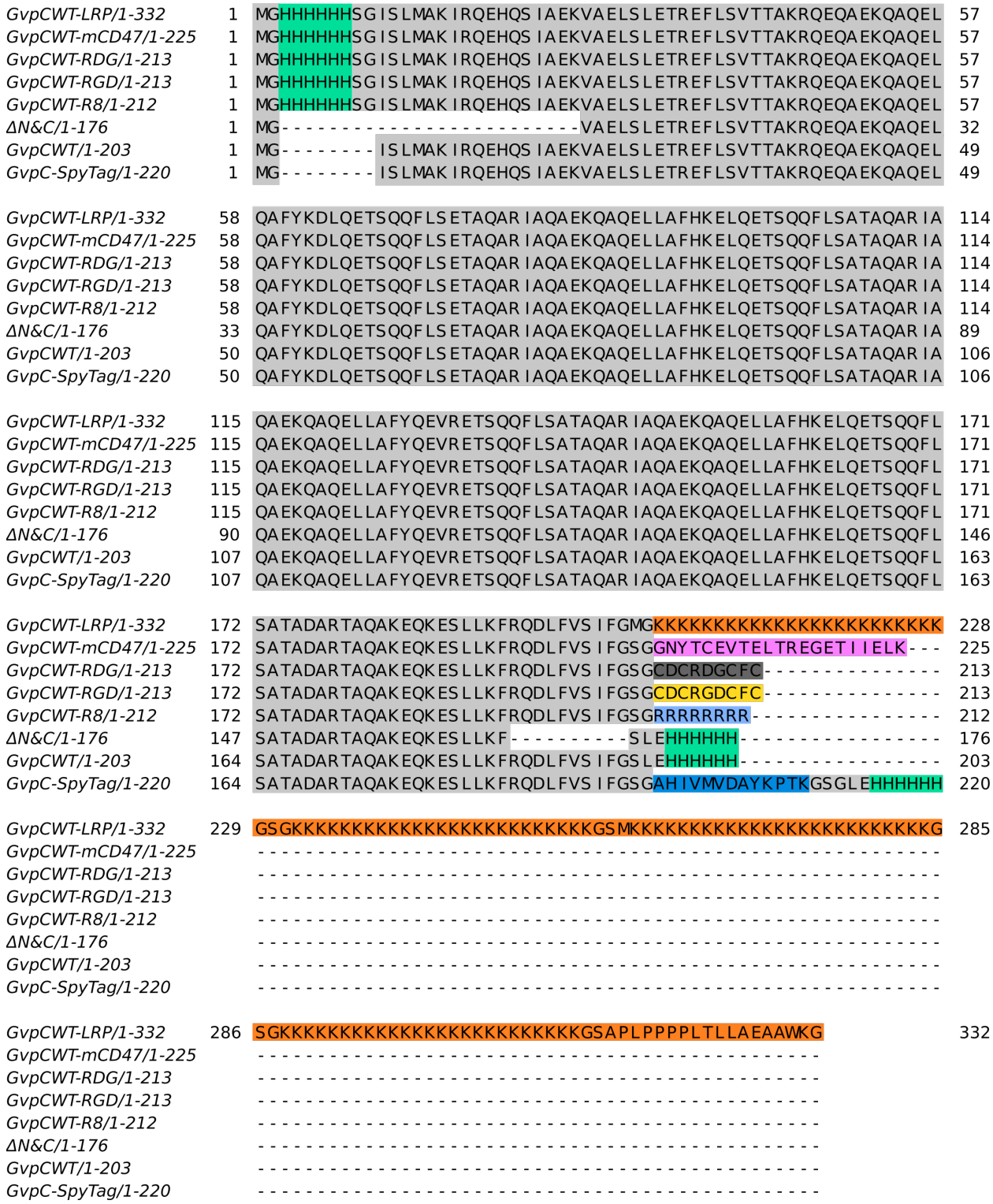

Figure S5: Clustal Omega sequence alignment of all the genetically engineered GvpC proteins used in our study. Colors highlight important features and are set to match the schematic illustration in Figure 5a.

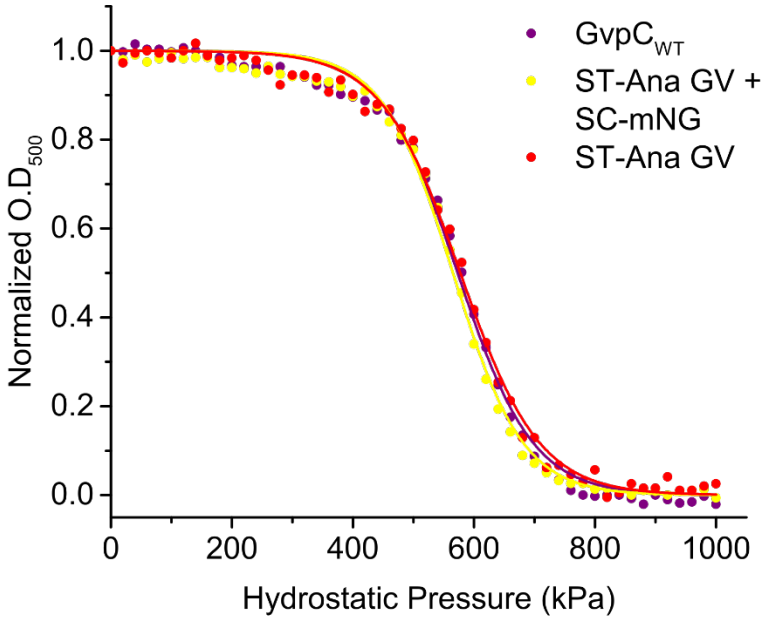

GV Variants	Midpoint of Collapse (P_c) (kPa)	P_c (SEM) (kPa)	ΔP (kPa)	ΔP (SEM) (kPa)	Adj. R-Square
GvpC$_{WT}$	572.84	2.33	62.00	2.05	0.996
ST-Ana GV + SC-mNG	565.13	2.18	57.70	1.92	0.996
ST-Ana GV	577.31	2.29	65.09	2.01	0.996

Figure S6: Optical density measurements of engineered Ana GVs as a function of hydrostatic pressure. The data was fitted with the Boltzmann sigmoid function $f(p) = \left(1 + e^{(p-p_c)/\Delta p}\right)^{-1}$ and the table provides the midpoint of collapse as well as other fit parameters and R^2 values. The data show that the collapse profile is unaltered even after reacting the ST-GVs with SC-mNG fluorescent protein.

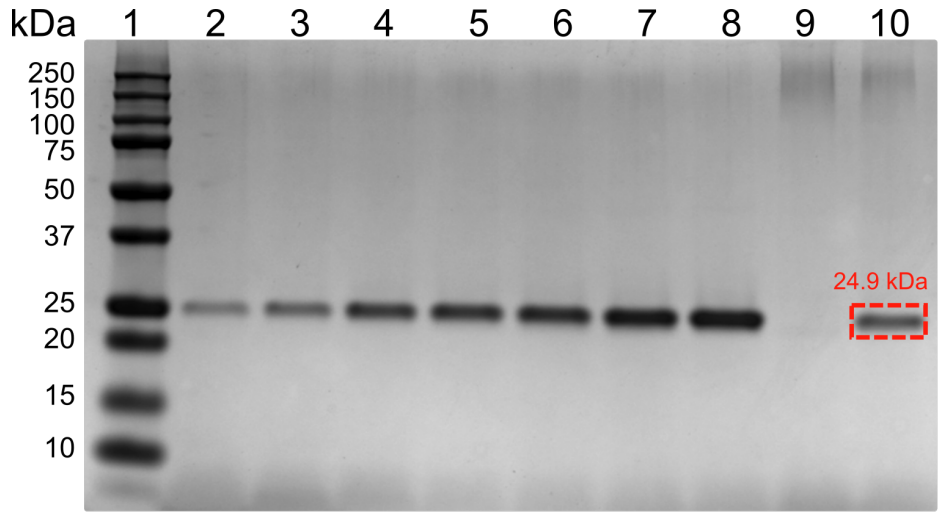

Lane	Sample
1	Ladder
2	GvpC-ST (100ng)
3	GvpC-ST (200ng)
4	GvpC-ST (400ng)
5	GvpC-ST (500ng)
6	GvpC-ST (600ng)
7	GvpC-ST (800ng)
8	GvpC-ST (1000ng)
9	ΔGvpC Ana GVs (OD: 7.8)
10	ST-Ana GVs (OD: 3.0)

Figure S7: SDS-PAGE quantification of SpyTag functionalities on the surface of engineered Ana GVs. Comparison of ST-Ana GVs (lane 10) against a standard curve comprising GvpC-ST concentrations ranging from 100-1000 ng (lanes 2-8) shows that each modified GV has ~ 1000 SpyTag functionalities. Stripped Ana GVs used for GvpC-ST re-addition (lane 9) have negligible amount of native GvpC.

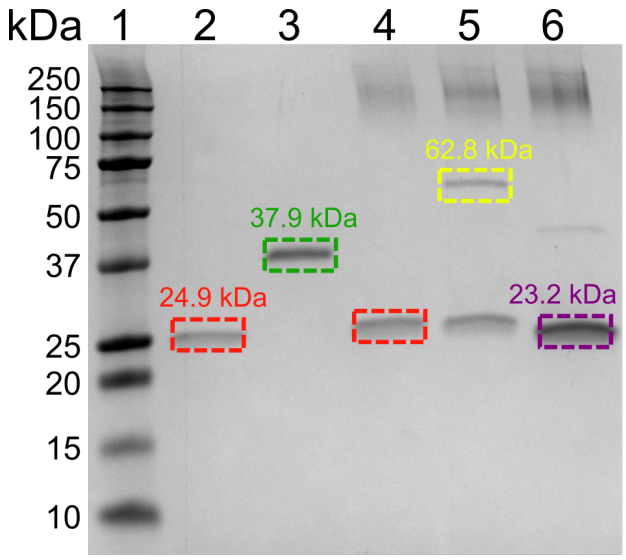

Lane	Sample
1	Ladder
2	GvpC-ST (24.9 kDa)
3	SC-mNG (37.9 kDa)
4	ST-Ana GVs (OD:3)
5	ST-Ana GVs (OD: 3) + SC-mNG (62.8 kDa)
6	$GvpC_{WT}$ Ana GVs (OD: 6) + SC-mNG

Figure S8: SDS-PAGE analysis confirms SpyTag-SpyCatcher bond formation (yellow) upon a one-hour incubation of ST-GVs having an outer layer of GvpC-SpyTag (red) with SpyCatcher-mNeonGreen (green). Incubation of Ana GVs containing an outer layer of WT-GvpC (purple) with SC-mNG, followed by buoyancy purification to remove unreacted fluorescent molecules results in GVs that are not fluorescent as shown in Figure 5g (left bottom panel). This also highlights the specificity of the SpyTag-SpyCatcher reaction and confirms that all the unreacted fluorescent molecules are completely removed during buoyancy purification.